

Inverse Photonuclear Reactions $N^{14}(p,\gamma)O^{15}$ and $N^{15}(p,\gamma)O^{16}$ in the Region of the Giant Resonance*

S. G. COHEN,† P. S. FISHER,‡ AND E. K. WARBURTON

Palmer Physical Laboratory, Princeton University, Princeton, New Jersey

(Received September 28, 1960)

The 90° yield of γ rays to the O^{16} ground state from the $N^{14}(p,\gamma)O^{15}$ reaction has been measured for proton energies between 12 and 19.5 Mev covering the region of excitation in O^{15} between 18 and 25 Mev. The excitation curve is quite flat (with $d\sigma/d\Omega$ at $90^\circ \approx 16 \mu b/4\pi$ sr), and shows little evidence of the giant resonance. The results for O^{15} are compared to those for N^{15} obtained by Jacobs and Stephens by means of the $N^{15}(\gamma,p)C^{14}$ reaction. The 90° yield of γ rays to the O^{16} ground state from the $N^{15}(p,\gamma)O^{16}$ reaction has been measured for proton energies between 10 and 15 Mev, corresponding to O^{16} excitation energies between 21 and 26 Mev. The excitation curve shows two large resonances peaked at 21.8 and 24.7 Mev with integral total cross sections of about 0.27 Mev-mb each if no background is assumed. The O^{16} results are compared to theoretical calculations of Elliott and Flowers and of others.

I. INTRODUCTION

RECENTLY, interest has arisen in the study of the giant-resonance region of nuclear excitation by means of inverse photonuclear reactions.¹⁻⁴ The (γ,p_0) and (p,γ_0) reactions, where p_0 and γ_0 represent transitions to the ground state of the residual nucleus, are related by the principle of detailed balancing. Thus, these two reactions should show a similar energy dependence in the region of the giant resonance.

There are several reasons why the inverse photo-reaction can be expected to be important—but not all important—in future investigations of the giant resonance. Opportunities for study of the giant resonance are extended by use of the (p,γ) reaction since the resonance may be studied for those excited nuclei whose ground states are unstable, and which are therefore unsuitable as targets for use in the (γ,p_0) reaction. A study of the (p,γ_0) reaction induced by monoenergetic protons is, *ipso facto*, capable of yielding detailed information more readily than the conventional study of (γ,p_0) reactions by means of a bremsstrahlung beam. On the other hand, the proton width of the giant resonance for the ground state of the $A-1$ nucleus is not expected to be an especially fundamental quantity. A complete study of the giant resonance phenomenon must, in fact, include investigations of all the particle widths of the giant resonance. For this purpose the photonuclear reaction cannot very well be replaced. However, observations on the capture gamma rays emitted to excited states of the residual nucleus can be

made with the (p,γ) reaction. Thus, it provides a direct method of studying questions such as whether or not there exist giant resonances built on the low-lying excited states as well as the ground state.

The (p,γ) investigations¹⁻³ of the giant resonance regions of Be^8 and C^{12} could be made using proton energies less than 12 Mev since the $Li^7(p,\gamma)Be^8$ and $B^{11}(p,\gamma)C^{12}$ reactions have high Q values (17.25 and 15.95 Mev, respectively) and the giant resonances are at about 22 Mev in these nuclei. At this laboratory the aim is to investigate inverse photo-proton reactions in cases involving lower Q values or for excitation above the giant resonance and thus at excitation energies above those accessible with tandem Van de Graaffs. For this purpose, variable proton energies up to 19.5 Mev are available from the Princeton synchrocyclotron.

The work reported herein is confined to measurements of differential cross sections at 90° as a function of excitation energy in the giant resonance region. The $N^{14}(p,\gamma)O^{15}$ and $N^{15}(p,\gamma)O^{16}$ reactions were investigated. A brief report of this work has appeared previously.⁵

The $N^{14}(p,\gamma)O^{15}$ reaction has a Q value of 7.30 Mev, so that it was expected that the giant resonance would be excited for incident proton energies around 15 Mev. Therefore, the reaction was explored for incident proton energies between 12 and 19.5 Mev. The ground state of O^{15} is unstable, and so the $O^{15}(p,\gamma)N^{14}$ reaction has not been investigated. On the other hand, the photo-proton reaction $N^{15}(\gamma,p)C^{14}$ has been investigated,⁶ and since the giant resonances studied in these two reactions, are in mirror nuclei, it is expected that the two reactions will have features in common.

The $O^{16}(\gamma,p)N^{15}$ reaction has been extensively

* This work was supported by the U. S. Atomic Energy Commission and the Higgins Scientific Trust Fund.

† On leave from The Hebrew University, Jerusalem, Israel.

‡ Now at Clarendon Laboratory, Oxford, England.

¹ D. S. Gemmell, A. H. Morton, and E. W. Titterton, *Nuclear Phys.* **10**, 33 (1959).

² H. E. Gove, A. E. Litherland, and R. Batchelor, *Phys. Rev. Letters* **3**, 177 (1959).

³ N. W. Reay and N. M. Hintz, *Bull. Am. Phys. Soc.* **4**, 403 (1959).

⁴ S. G. Cohen, P. S. Fisher, and E. K. Warburton, *Phys. Rev. Letters* **3**, 433 (1959).

⁵ See reference 4. The present results contain a more careful appraisal of the gamma-ray detection efficiency than those of reference 4 and should be considered as superseding the previous report.

⁶ J. L. Rhodes and W. E. Stephens, *Phys. Rev.* **110**, 1415 (1958).

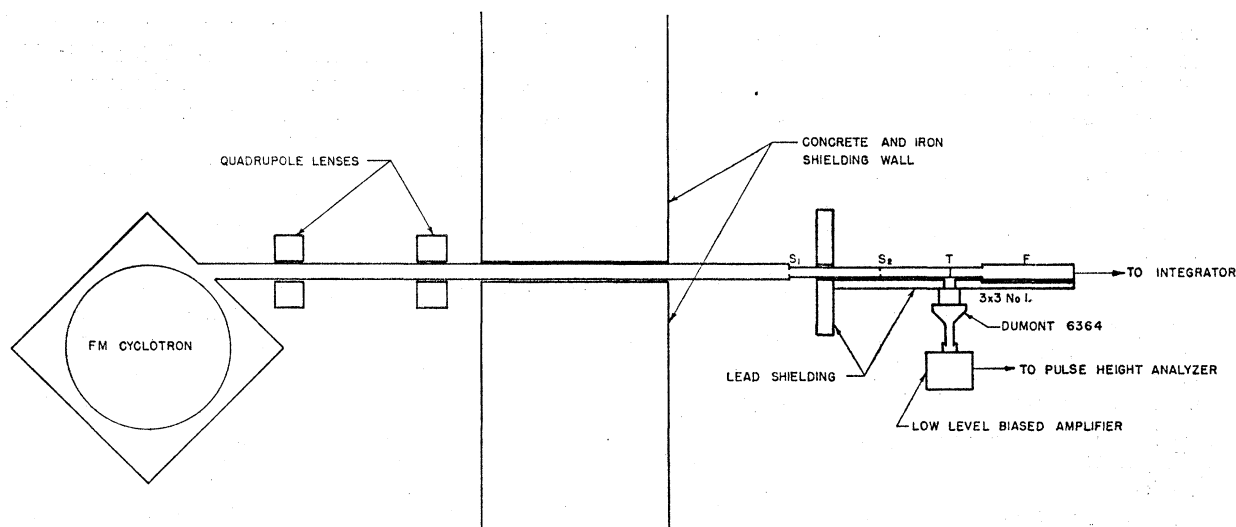


FIG. 1. Schematic view of the experimental arrangement. S_1 is a carbon collimator with a $\frac{1}{4}$ -in. aperture, S_2 is a similar collimator with $\frac{3}{8}$ -in. aperture. The target is designed by T , and the carbon lined Faraday cup by F .

studied,⁷⁻¹⁰ and shows evidence of structure from near threshold to about 27-Mev excitation in O^{16} with the giant resonance centered at ~ 23 Mev. In this work the $N^{15}(p, \gamma)O^{16}$ reaction ($Q=12.11$ Mev) was investigated for excitation energies between 21 and 26 Mev, the lower limit giving an overlap of several Mev with the energy region available to tandem Van de Graaffs. Such an accelerator has been used, in fact, in a recent study¹¹ of the $N^{15}(p, \gamma)O^{16}$ reaction with proton energies up to 8 Mev which corresponds to an O^{16} excitation energy of 19.6 Mev.

II. EXPERIMENTAL PROCEDURE

The general experimental arrangement is shown in Fig. 1. A 3 by 3 in. NaI(Tl) crystal, mounted on a 5-in. Dumont 6364 photomultiplier, was used as a detector for the high-energy γ rays. The crystal was placed at 90° to the proton beam and 7 cm from the target. The spectrum of pulse heights was displayed on a RIDL 200-channel analyzer.

Between 14.5 and 19.5 Mev, the energy of the proton beam was changed by varying the synchrocyclotron characteristics. To reach energies below 14.5 Mev a polyethylene absorber either 99 mg/cm² or 119 mg/cm² thick, was placed in the beam so as to extend the range of proton energies to lower values. The polyethylene absorber was placed just in front of collimator S_1 (see Fig. 1) which was about 60 cm in front of the target. A second collimator (S_2) served to define the proton

beam which was drastically scattered by the thickest (~ 5 -Mev energy loss) absorber used. The full energy width at half maximum of the unattenuated proton beam was about 150 kev, while the calculated energy spread due to straggling in the absorber was ~ 200 kev.

The whole beam tube, including the Faraday cup, was lined with graphite and the collimators were fabricated from graphite sheet. By this means the neutron background was kept to a minimum, since the (p, n) threshold in C^{12} is at 20 Mev. Although initially some attempts were made to shield the crystal from neutrons originating from the cyclotron, the target, and impurities in the graphite and polyethylene, it was difficult to shield efficiently with the detector close to the target, and in the final runs it was found advantageous to work without neutron shielding in the region of the detector. The proton beam impinging on the graphite and polyethylene produced a copious source of $C^{12}(p, p')C^{12}$ γ rays. The lead shielding shown in Fig. 1 was efficient enough so that, in the pulse-height region of interest, the background arose almost entirely from the target itself.

In order to see clearly the spectrum of high-energy capture γ rays of low intensity in the presence of pileup from a spectrum of high intensity background radiation, produced by lower energy γ rays and neutrons, it was found necessary to adopt several measures. The beam intensity was kept low to minimize pileup of small pulses in the detector and electronic circuits. The beam current varied with energy, being about $3 \times 10^{-6} \mu a$ at the lowest proton energy (9.5 Mev) with the thickest absorber and about $3 \times 10^{-4} \mu a$ at higher energies. A short clipped pulse (2×10^{-7} sec) was formed at the output of the photomultiplier and the pulses fed into a biased transistor preamplifier. In this way all pulses corresponding to a γ -ray energy of less than 10 Mev

⁷ L. Cohen, A. K. Mann, B. J. Patton, K. Reibel, W. E. Stephens, and E. J. Winhold, Phys. Rev. **104**, 108 (1956).

⁸ S. A. E. Johansson and B. Forkman, Arkiv Fysik **12**, 359 (1957).

⁹ C. Milone, S. Milone-Tamburino, R. Rinziivillo, A. Rubbino, and C. Tribuno, Nuovo cimento **7**, 729 (1958).

¹⁰ P. Brix and E. K. Maschke, Z. Physik **155**, 109 (1959).

¹¹ N. W. Tanner, G. C. Thomas, and W. E. Meyerhof, Nuovo cimento **14**, 257 (1959).

were excluded before the pulses were lengthened and fed to the pulse-height analyzer. The analyzer was gated to the beam pulse of the synchrocyclotron so as to remove the background pulses which were not prompt with respect to the beam.

The $N^{14}(p,\gamma)O^{15}$ reaction was investigated first. Melamine ($C_3N_6H_6$) suspended in polystyrene was used as a target material.¹² A target thickness of about 4.9 mg/cm² was used in most of the runs, corresponding to a proton energy loss of about 120 kev at 17.0 Mev. The background due to carbon was measured in separate runs using a polyethylene target containing the same amount of carbon as the melamine target. It was found that the background within 5 Mev of the pulse height corresponding to the full energy loss of the γ rays leading to the O^{15} ground state was due primarily to radiations—presumably fast neutrons—coming from the nitrogen in the target. No contribution from the $C^{12}(p,\gamma)N^{13}$ reaction was expected in this region because the Q value is only 1.94 Mev. For proton energies above its threshold, the $(J^\pi, T) = (1^+, 1)$, 15.1-Mev level of C^{12} was strongly excited and gave a prominent γ ray of this energy. This γ -ray line provided a convenient calibration in the high-energy region.

For the $N^{15}(p,\gamma)O^{16}$ investigation, N_2 gas enriched to 98.7% in N^{15} was used as a target. The gas was fed into a cylindrical cell 3.8 cm long, 1 cm in diameter, from an activated charcoal trap into which it had been absorbed at liquid nitrogen temperature. Observations were made with N_2 gas at a pressure of 930 mm Hg, corresponding to a proton energy loss of about 200 kev at 12 Mev. The end windows were of 0.0005-in. Mylar sheet, giving about 40-kev energy loss at $E_p = 12.0$ Mev. The background from the N^{14} in the N_2 gas and from the Mylar—which contains hydrogen, carbon, nitrogen, and oxygen—was negligible, within about 10 Mev of the pulse height corresponding to the full energy loss of the O^{16} ground-state capture γ rays. This was so because the $O^{16}(p,\gamma)F^{17}$ reaction has a Q value of only 0.60 Mev and because the cross section for the $N^{15}(p,\gamma)O^{16}$ reaction is considerably larger than that of the $N^{14}(p,\gamma)O^{15}$ reaction in the energy region studied (see Sec. III).

For both targets the total beam spread was about 200 kev without an absorber and 300 kev with an absorber. The beam energy was known to ± 200 kev.

The spectral response of the 3 by 3 in. NaI(Tl) crystal was determined by recording high-energy γ spectra from the $Li^7(p,\gamma)Be^8$ and $C^{12}(p,p')C^{12}$ reactions. The former reaction was produced by 500-kev protons from the Brookhaven National Laboratory Van de Graaff accelerator. At this proton energy, γ rays of 17.5 and 14.6 Mev were produced from a thick Li^7 target. For cyclotron energies above 17 Mev, the $C^{12}(p,p')C^{12}$ reaction produced a copious source of 15.1-Mev γ rays.

¹² We would like to thank Dr. R. W. Detenbeck for preparing the melamine targets.

The spectral shapes obtained were similar to published curves for γ rays in the range 12–30 Mev.^{13,14} The spectral response is known to vary very little for γ -ray energies between 15 and 30 Mev¹⁴ and so was assumed constant in the present work.

For a point source situated on the cylindrical axis of a 3 by 3 in. NaI(Tl) scintillation crystal and 7 cm from the front face, the absolute γ -ray detection efficiency is calculated¹⁵ to be 2.8–3.0% for γ -ray energies of 20 and 28 Mev, respectively. In the present experiments this efficiency was corrected for absorption in the brass wall of the target chamber ($\sim 10\%$), extension of the target area in the case of the gas target ($\sim 5\%$), and absorption in the lead collimator placed between the crystal and target ($\sim 16\%$). The latter two corrections were obtained from measurements made using the $Li^7(p,\gamma)Be^8$ γ rays and low-energy γ rays from radioactive sources. In obtaining the differential cross section from the $N^{14}(p,\gamma)O^{15}$ and $N^{15}(p,\gamma)O^{16}$ γ -ray spectra only the high pulse-height portion of the spectra were summed. The fraction of the total number of counts in this sum was estimated from the spectral response

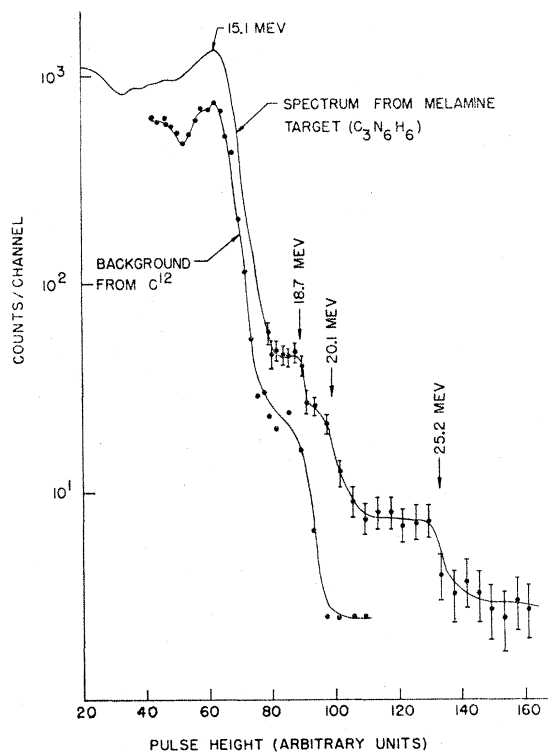


FIG. 2. Gamma-ray pulse height distribution produced by bombardment of a melamine target with 19.3-Mev protons. The spectrum produced by bombardment of a polyethylene target is also shown.

¹³ M. M. Wolff, University of Pennsylvania Technical Report No. 4, May, 1958 (unpublished).

¹⁴ H. W. Koch and J. M. Wyckoff, National Bureau of Standards Report No. 5866 (unpublished).

¹⁵ E. A. Wolicki, R. Jastrow, and F. Brooks, Naval Research Laboratory Report 4833, 1956 (unpublished).

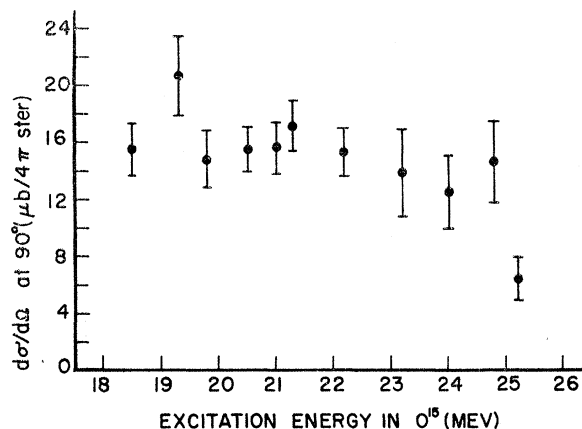


FIG. 3. The differential cross section at 90° for the γ rays leading to the ground state of O^{15} from the $N^{14}(p, \gamma)O^{15}$ reaction. If the γ rays have an isotropic distribution relative to the proton beam the ordinate scale gives the total cross section.

curves obtained for $Li^7(p, \gamma)Be^8$ and $C^{12}(p, p')C^{12}$. (For instance, 37% of the counts were estimated to be within 25% of the maximum pulse height.) The net efficiency was the product of the total efficiency,¹⁵ the correction factors mentioned above, and the fraction of counts which were summed. This efficiency varied between 0.3 and 0.6% and had an estimated uncertainty of 35%, mostly from the uncertainty in the shape of the pulse-height-curve.

III. RESULTS

A. $N^{14}(p, \gamma_0)O^{15}$ Reaction

Figure 2 shows a pulse-height spectrum of γ rays from the melamine target taken at an incident proton energy of 19.3 Mev. The background spectrum obtained with a polyethylene target is also shown. The spectra of Fig. 2 represent results obtained in two hour runs with an average beam current of $3 \times 10^{-4} \mu a$. The 15.1-Mev peak due to the excitation of the C^{12} 15.1-Mev level by (p, p') is clearly seen. The plateau with a steep drop at 25.2 Mev at the high energy end must be attributed to capture γ rays to the ground state of O^{15} . The effects of pileup on the spectrum near this plateau were shown to be negligible by repeating this spectrum with $\sim \frac{1}{3}$ the beam intensity. There is some indication in the melamine spectrum of γ rays of about 20.1 Mev which is the energy expected for capture γ rays leading to the first two excited states of O^{15} at 5.20 and 5.25 Mev. The structure at 18.7 Mev most probably corresponds to capture γ rays leading to the third excited state (6.15 Mev) of O^{15} and to capture γ rays from the $C^{12}(p, \gamma_0)N^{13}$ reaction—for which the γ -ray energy should be 18.8 Mev. It was not possible to identify transitions to excited states at lower proton energies with any certainty—presumably because of the higher background in the γ -ray energy region of interest—so that no attempt was made to obtain excitation curves for capture γ rays other than to the O^{15} ground state. At

each proton energy the energy measured for the highest group in the spectrum checked very well with that expected for capture γ rays to the O^{15} ground state.

In estimating the relative intensities of γ_0 at the various proton energies, a background in the region of the peak energy was subtracted which was consistent with the general shape of the pulse spectrum above and below the peak, but which left correctly shaped spectrum. The counts included within a given pulse-height range of the maximum pulse height were then summed. The counting statistics were calculated from this sum and an estimate of the uncertainty in the background subtraction.

Figure 3 shows the 90° yield of $N^{14}(p, \gamma_0)O^{15}$ as a function of excitation in O^{15} . The energy scale is also the capture γ -ray energy and is related to the proton energy by $E_\gamma = (14/15)E_p + 7.30$ Mev. The error bars are the estimated relative errors and do not include the uncertainty in the differential cross section. The differential cross section has an estimated uncertainty of 40% due mostly to the uncertainty in the net efficiency (see Sec. II), the integrated beam intensity, and the target thickness.

B. $N^{15}(p, \gamma_0)O^{16}$ Reaction

In Fig. 4 is shown a pulse-height spectrum of γ rays obtained at 90° to the proton beam from bombardment of the N^{15} gas with protons having an energy of 10.3 Mev at the center of the gas target. The capture γ rays to the ground state of O^{16} should have an energy of 21.7

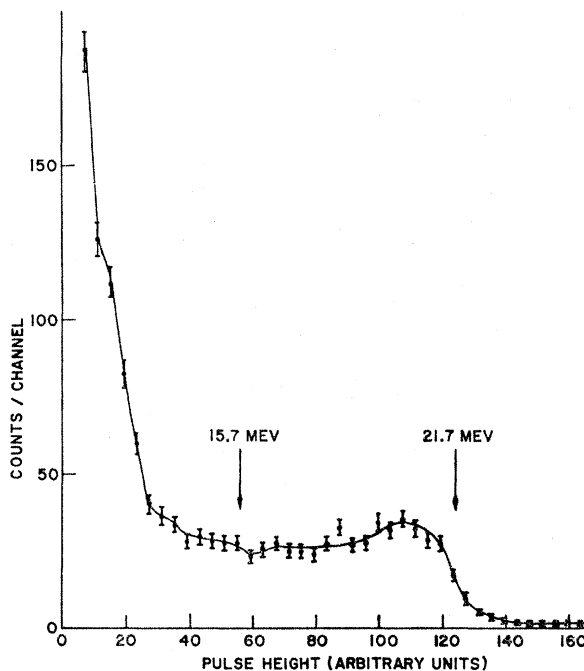


FIG. 4. Gamma-ray pulse height distribution produced by bombardment of an N^{15} gas target with 10.3-Mev protons.

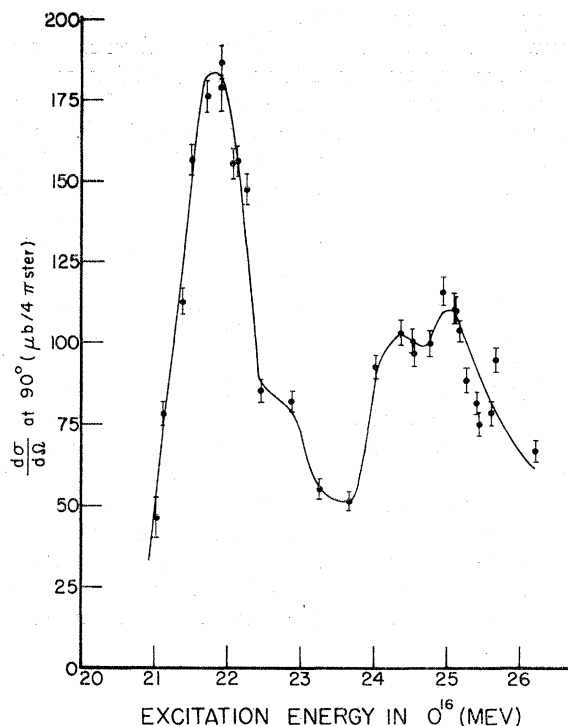


FIG. 5. The differential cross section at 90° for the γ rays leading to the ground state of O^{16} from the $N^{15}(p,\gamma)O^{16}$ reaction. If the γ rays have an isotropic distribution relative to the proton beam, then the ordinate scale gives the total cross section.

Mev at $E_p=10.3$ Mev. The structure due to these γ rays is clearly visible in Fig. 4. Capture γ rays to excited states of O^{16} would have energies of 15.7 Mev or less. From the various spectra it was apparent that these transitions were excited but no reliable estimates could be made of their intensity because of the rapidly rising background, and no attempt was made to measure an excitation function for transitions to excited states. In analyzing the data for the variation of cross section with energy, a background was subtracted on the assumption that the flat background observed at energies above the maximum energy of the ground-state capture γ rays continued in the same way at least 5 Mev below the maximum energy. After the background subtraction, the spectra were analyzed to obtain the total number of counts due to $N^{15}(p,\gamma_0)O^{16}$ in the same manner as was done for the $N^{14}(p,\gamma_0)O^{15}$ reaction.

Figure 5 shows the 90° yield of $N^{15}(p,\gamma_0)O^{16}$ as a function of excitation energy in O^{16} . As in Fig. 4 the error bars are the estimated relative errors. The differential cross section scale is thought to be accurate to 40%.

IV. DISCUSSION OF RESULTS

A. $N^{14}(p,\gamma_0)O^{15}$ Reaction

In Fig. 6(a) is shown the total cross section for the $O^{15}(\gamma,p_0)N^{14}$ reaction as a function of γ -ray energy (or

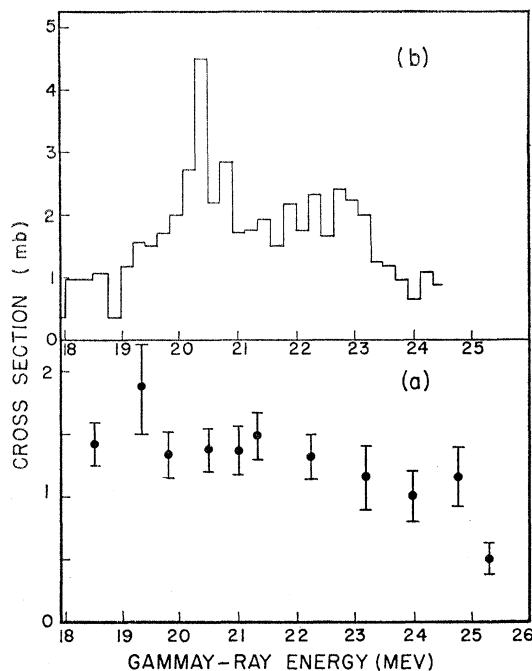


FIG. 6. Comparison of the $O^{15}(\gamma,p_0)N^{14}$ and $N^{15}(\gamma,p_0)C^{14}$ reactions. The lower curve [Fig. 6(a)] shows the total cross section versus γ -ray energy (or excitation energy in O^{15}) for the $O^{15}(\gamma,p_0)N^{14}$ reaction obtained by detailed balance from the $N^{14}(p,\gamma_0)O^{15}$ yield curve of Fig. 3 assuming an isotropic distribution of the γ rays relative to the proton beam. The upper curve [Fig. 6(b)] shows the total cross section versus γ -ray energy (or excitation energy in N^{15}) for the $N^{15}(p,\gamma_0)C^{14}$ reaction (reference 7).

excitation energy in O^{15}). Figure 6(a) was obtained by detailed balance from the 90° differential cross section of Fig. 3 assuming the γ rays in the $N^{14}(p,\gamma_0)O^{15}$ reaction have an isotropic distribution relative to the proton beam. It is expected that this assumption introduces an error of at most 20% in the total cross section¹⁶ so that the total cross section scale of Fig. 6(a) is estimated to have an uncertainty of 45%.

Figure 6(b) was taken from Jacobs and Stephens⁷ and shows their results for the $N^{15}(\gamma,p_0)C^{14}$ reaction cross section as a function of γ -ray energy (or excitation energy in N^{15}). The $N^{15}(\gamma,p_0)C^{14}$ excitation curve indicates that the giant resonance in N^{15} is centered at ~ 21.5 Mev with a width at half-maximum of ~ 5 Mev; while the $O^{15}(\gamma,p_0)N^{14}$ excitation curve is quite flat with only a falloff at 25 Mev to suggest the giant resonance of O^{15} .

As long as nuclear forces are charge symmetric the mirror nuclei, O^{15} and N^{15} , are expected to have giant resonances of similar shapes. In spite of this, the difference between the curves of Figs. 6(a) and 6(b) is

¹⁶ For instance, for a γ -ray distribution of the form $1+A\cos^2\theta$ with $1 \geq A \geq -1$ and for the geometry used in the present experiment, the correction factor for the total cross section of Fig. 6(a) would be between 1.15 and 0.80. Actually, the experimental and theoretical evidence is that $0 \leq A \leq -1$ for (γ,p) reactions in the giant resonance region; therefore, it is most probable that the $O^{15}(\gamma,p_0)N^{14}$ cross section of Fig. 6(a) errs on the high side.

not surprising since both show excitation curves for a particular mode, while the giant resonance is associated with the total γ -ray absorption cross section. As an example of the differences to be expected between these two curves consider the sharp peak at 20.5 Mev in the $N^{15}(\gamma, p_0)C^{14}$ excitation curve [Fig. 6(b)]. The nuclear state (or states) which is responsible for this peak will also be present in O^{15} and it is possible that the high point at 19.3 Mev in the $O^{15}(\gamma, p_0)N^{14}$ excitation curve [Fig. 6(a)] is associated with this state (or states). That is, the difference in excitation energies (20.5–19.3 = 1.2 Mev) is about that expected for the difference in excitation energy between mirror states at ~ 20 -Mev excitation in N^{15} - O^{15} . However, it is also possible that the state (or states) in question has a negligibly small proton width for the N^{14} ground state. This would be true, for example, if this level had isotopic spin $T = \frac{3}{2}$ in which case it could decay by nucleon emission to the $(J^\pi, T) = (0^+, 1)$, C^{14} ground state (or N^{14} first excited state), but not to the $(1^+, 0)$, N^{14} ground state.

The N^{15} and O^{15} giant resonances can be compared in more detail by integrating the cross sections of Fig. 6 over the giant resonance region. From Fig. 6(a) the integrated cross section for the $O^{15}(\gamma, p_0)N^{14}$ reaction between 18.7 and 24.6 Mev is found to be 7.7 Mev-mb; while Jacobs and Stephens obtained an integrated cross section of 10.6 Mev-mb for the same photon energy interval in the $N^{15}(\gamma, p_0)C^{14}$ reaction [Fig. 6(b)].

There is a direct relation between the cross sections for the $N^{15}(\gamma, p_0)C^{14}$ and $O^{15}(\gamma, p_1)N^{14}$ reactions if charge independence of nuclear forces is assumed and if the γ -ray absorption is pure $E1$. Here p_1 represents proton transitions to the 2.31-Mev first excited state of N^{14} which is the $M_T = 0$ member of the $(0^+, 1)$ isotopic-spin triplet of which the C^{14} ground state is the $M_T = 1$ member. As pointed out by Morpurgo,¹⁷ $E1$ rates between corresponding states in mirror nuclei are equal as long as nuclear forces are charge independent. In this case, the cross-section ratio of the $N^{15}(\gamma, p_0)C^{14}$ and $O^{15}(\gamma, p_1)N^{14}$ reactions will be determined by the relative probability of proton emission into the final mass-14 state. The $N^{15}(\gamma, p_0)C^{14}$ and $O^{15}(\gamma, p_1)N^{14}$ Q values are –10.21 and –9.61 Mev respectively. The small difference between these Q values will be neglected in the following discussion; that is, kinematical factors (which would slightly favor the $O^{15} + \gamma$ reaction) will be neglected. In this case, the cross section ratio of the $N^{15}(\gamma, p_0)C^{14}$ and $O^{15}(\gamma, p_1)N^{14}$ reactions proceeding through corresponding intermediate states (excited states in N^{15} and O^{15} with $M_T = \frac{1}{2}$ and $-\frac{1}{2}$, respectively, will be equal to the ratio of the isotopic-spin factors $\langle T_p \frac{1}{2} M_T - \frac{1}{2} | T M_T \rangle^2$, where T_p and M_T are the isotopic spin and z component of isotopic spin of the final state (the C^{14} ground state and N^{14} first-excited state, respectively). This ratio is 2 for $T = \frac{1}{2}$ and $\frac{1}{2}$ for $T = \frac{3}{2}$, so that the integrated cross section for the $O^{15}(\gamma, p_1)N^{14}$

reaction between γ -ray energies of 18.7 and 24.6 Mev is inferred from the $N^{15}(\gamma, p_0)C^{14}$ cross-section measurement to be between 5.3 and 21.2 Mev-mb if isotopic spin is a good quantum number in the giant resonance region of mass 15 and if the photonuclear absorption into this region of excitation is electric dipole. This integrated cross section leads to a maximum value for the ratio,

$$\int_{18.7}^{24.6} \sigma_0 dE / \int_{18.7}^{24.6} \sigma_1 dE,$$

of ~ 1.5 which occurs when the (γ, p) cross section in the integrated energy range is entirely due to $T = \frac{1}{2}$ states. In this ratio σ_0 and σ_1 represent the cross sections for the $O^{15}(\gamma, p_0)N^{14}$ and $O^{15}(\gamma, p_1)N^{14}$ reactions, respectively. This cross-section ratio provides one test for any detailed calculation of the mass-15 photonuclear effect. For instance, if the (γ, p) or (p, γ) reactions in question proceed via the compound nucleus mechanism then, neglecting kinematical factors, it can be shown from the limits on the integrated cross section ratio given above that the ratio of the average effective proton reduced widths in the range of excitation 18.7–24.6 Mev in O^{15} satisfies the inequality

$$\frac{1}{9} \leq \frac{\langle \theta_{p0}^2 \rangle}{\langle \theta_{p1}^2 \rangle} \leq 1.0, \quad (1)$$

where we have used the fact that θ_{p0}^2 is zero for $T = \frac{3}{2}$ states in O^{15} . If the assumptions made in obtaining Eq. (1) are valid, it appears that the mass 15 giant resonance, if it is centered at ~ 22 Mev, has the N^{14} first-excited state as parent to a greater extent than the N^{14} ground state. It might be fruitful to compare this ratio, and any other details which might be gleaned from the $N^{15}(\gamma, p)C^{14}$ results of Jacobs and Stephens⁷ and the present $N^{14}(p, \gamma)O^{15}$ results, with the mass 15 shell model calculations of Halbert and French.¹⁸

The integrated cross section for electric dipole absorption in the nuclear photoeffect is given as¹⁹

$$\int \sigma dE = 60(NZ/A)(1 + 0.8x) \text{ Mev-mb}, \quad (2)$$

where x is the fraction of the neutron-proton interaction which has an exchange character. For N^{15} or O^{15} this has the value $224(1 + 0.8x)$ Mev-mb, with limiting values of 224 and 403 Mev-mb for x between 0 and 1. Thus it is clear that the $O^{15}(\gamma, p_0)N^{14}$ cross section—integrated from 18.7 to 24.6 Mev—is only a small fraction of the dipole sum. This is not surprising since the O^{15} ground state has nine p^{10} parents in N^{14} and five p^{10} parents in O^{14} . Thus it should be expected that the

¹⁸ E. C. Halbert and J. B. French, Phys. Rev. **105**, 1563 (1957). These authors did not publish their results for N^{15} or O^{15} levels above 15 Mev, but state that the wave functions are available for study of the N^{15} (and thus O^{15}) photodisintegration.

¹⁹ J. S. Levinger and H. A. Bethe, Phys. Rev. **78**, 115 (1950).

¹⁷ G. Morpurgo, Phys. Rev. **114**, 1075 (1959).

O^{15} giant resonance will have many competing modes of nucleon emission.²⁰

B. $N^{15}(\rho, \gamma_0)O^{16}$ Reaction

The $N^{15}(\rho, \gamma_0)O^{16}$ excitation curve of Fig. 5 shows two peaks centered at 21.8 and 24.7 Mev. The 24.7-Mev peak shows some evidence of structure, but the statistical errors are such that this is not established for certain. These results can be compared to those for the photo-nuclear reaction⁷⁻¹⁰ $O^{16}(\gamma, p_0)N^{15}$ by applying the principle of detailed balancing. It is found that $\sigma(\gamma, p_0) = 77\sigma(\rho, \gamma_0)$ to better than 3% throughout the excitation energy range of Fig. 5. This conversion factor gives an $O^{16}(\gamma, p_0)N^{15}$ 90° differential cross section of 14 mb/4 π sr for the peak at 21.8 Mev in Fig. 5 and an $O^{16}(\gamma, p_0)N^{15}$ integrated cross section of 41 Mev-mb/4 π sr for the γ -ray energy range 21-26.5 Mev. This integrated cross section is divided equally between the intervals 21-23.5 Mev and 23.5-26.5 Mev.

The measured (γ, p_0) angular distributions^{8,10} can be used to obtain total cross sections from the differential cross sections of Fig. 5. The (γ, p_0) angular distributions have a maximum near 90°^{8,10} so that a total cross section obtained by integrating the differential value observed at 90° over all directions (as was done in Fig. 5) is expected to be too large by 10-15% for the geometry used in this experiment.

The present results are in excellent qualitative agreement with the $O^{16}(\gamma, p_0)N^{15}$ results⁷⁻¹⁰ obtained with bremsstrahlung beams both as to the cross section and the general shape of the giant resonance. There can be no doubt that the $O^{16}(\gamma, p_0)N^{15}$ excitation curve in the giant resonance region is split into two distinct peaks, although there is some disagreement as to the energy positions and shapes of these peaks. However, this disagreement is not serious in view of the accuracy of the various measurements. For example, it is possible that the 90° excitation curve of Fig. 5 differs significantly from the total cross-section excitation curve because of a strong energy dependence of the (γ, p_0) angular distribution function.

The theoretical work of Elliott and Flowers,²¹ of Pal,²² and of Brown and Bolsterli²³ show that the general features of the O^{16} giant resonance agree with the Wilkinson²⁴ model which explains the giant resonance

²⁰ An unpublished manuscript of this paper was circulated privately and included in the Proceedings of the Karlsruhe Photo-nuclear Conference (1960). In this manuscript an argument was presented to the effect that the giant resonance of mirror nuclei with $T = \frac{1}{2}$ ground states should be mostly due to $T = \frac{1}{2}$ states. As was kindly pointed out to the authors by G. Morpurgo, the main assumption which lead to this conclusion was unjustified and so, therefore, is the conclusion itself.

²¹ J. P. Elliott and B. H. Flowers, Proc. Roy. Soc. (London) **A242**, 57 (1957).

²² M. K. Pal (private communication); M. K. Pal and Y. C. Lee, Bull. Am. Phys. Soc. **4**, 406 (1959); S. Fallieros, R. A. Ferrell, and M. K. Pal, Nuclear Phys. **15**, 363 (1960).

²³ G. E. Brown and M. Bolsterli, Phys. Rev. Letters **3**, 472 (1959).

²⁴ D. H. Wilkinson, Physica **22**, 1039 (1956).

in terms of single-particle excitations of the ground state. Before the work of Brown and Bolsterli²³ there was thought to be a conflict between the experimentally known spacings of single-particle states and the considerably larger spacings required to identify the nuclear giant resonance with single-particle excitations. Brown and Bolsterli removed this difficulty by showing in a quite general manner that the single-particle state carrying the bulk of the dipole strength would, by virtue of its symmetry, be pushed up in energy so as to appear at an excitation compatible with the known position of the nuclear giant resonance. The spin-orbit interaction was neglected in this work. Pal²² calculated the effects of the spin-orbit interaction in O^{16} by calculating the interaction of the dipole state (i.e., the state responsible for the giant resonance in the Brown-Bolsterli treatment) with the $(1^-, 1)$ single-particle state generated by applying the operator $\sum_i (\mathbf{r}_i \times \boldsymbol{\sigma}_i) \cdot \boldsymbol{\tau}_3(i)$ to the O^{16} ground state. He showed that the spin-orbit interaction pushed this state closer to the dipole state and caused considerable mixing of the properties of these two states, but left the other three $p^{-1}d$ and $p^{-1}2s$ states essentially unchanged. The result was a splitting of the giant resonance in agreement with experiment. Previous to the work of Brown and Bolsterli and of Pal, Elliott, and Flowers²¹ had done a conventional shell-model calculation of the odd-parity states of O^{16} arising from the $p^{-1}d$ and $p^{-1}2s$ configurations. They obtained excitation energies and wave functions for the five $(1^-, 1)$ states of these configurations. The two highest states were predicted to be at excitation energies of 22.6 and 25.2 Mev and were predicted to have almost all of the dipole sum in O^{16} . It would then be expected that these two states would be the same as those generated by Pal; and, in actual fact, the wave functions obtained by Pal for the two $(1^-, 1)$ states responsible for the giant resonance in O^{16} are quite similar to the wave functions of the 22.6- and 25.2-Mev states of Elliott and Flowers. Thus, the work of Brown and Bolsterli and of Pal gives us a qualitative explanation of the results of Elliott and Flowers.

The wave functions of Elliott and Flowers give the radiative widths: $\Gamma_\gamma = 5.8$ ev and 12.0 ev, for the upper and lower $(1^-, 1)$ states, respectively; while the results of Pal indicate that the upper state has a radiative width approximately twice as large as the lower state. As pointed out by Elliott and Flowers, these single-particle states will be mixed with a multitude of $J^\pi = 1^-$ states arising from more highly excited states. This phenomenon will give rise to fine structure in the giant resonance and could be the explanation for the structure in the 24.7-Mev peak, which is suggested by the present results (Fig. 5). However, the total dipole absorption to all states sharing the properties of a given single-particle state is still expected to be that predicted for the single-particle state in the absence of mixing.

Assuming compound nucleus formation, the Breit-

Wigner one level formula can be used to estimate the $E1$ radiative widths of the two components of the O^{16} giant resonance shown in Fig. 5. For the 21.8-Mev peak in $O^{16}(\gamma, p_0)N^{15}$, the result is

$$\Gamma_\gamma(21.8) \simeq 0.042(\Gamma/\Gamma_{p_0}) \int \sigma dE (\text{in Mev-mb}) \text{ kev}, \quad (3)$$

where the widths refer to the O^{16} 21.8-Mev resonance, Γ_γ and Γ_{p_0} are the partial widths for decay to the O^{16} and N^{15} ground states, and Γ is the total width. (Because of the mixing of the single-particle state with more highly excited configurations, the total width Γ cannot be identified with the measured width of the 21.8-Mev resonance.) The $O^{16}(\gamma, p_0)N^{15}$ integrated cross section for the 21.8-Mev resonance is estimated as 20.5 Mev-mb, which is the value obtained from the excitation curve of Fig. 5 for the range 21–23.5 Mev. This leads to an overestimation of $\int \sigma dE$ since it assumes zero background to the resonance and neglects the correction for the anisotropy of the (p, γ_0) angular distribution. On the other hand, integrating from 21 to 23.5 Mev ignores the contribution of more distant states which have mixed with the single-particle state. The ratio Γ/Γ_{p_0} cannot be obtained from the present experiment. To obtain this ratio it is assumed that $\Gamma = \Gamma_p + \Gamma_n$ since other decay modes are not expected to be important. The ratio of the integrated (γ, n) and (γ, p) cross sections for O^{16} excitations in the range 21–23.5 Mev is approximately 1,⁸ so that $\Gamma_p \simeq \Gamma_n$. Finally, the branching ratio to the N^{15} ground state in the $O^{16}(\gamma, p)N^{15}$ reaction in the energy region 21–23.5 Mev is taken as 77%, the average of the measurements

of Johansson and Forkman⁸ and of Milone *et al.*⁹ The result is $(\Gamma/\Gamma_{p_0}) \simeq 2.6$, which gives

$$\Gamma_\gamma(21.8) \simeq 2.2 \text{ kev}. \quad (4)$$

Using the same procedure, the radiative width for the 24.7-Mev resonance, obtained by integrating the cross section of Fig. 5 from 23 to 26.5 Mev is estimated to be in the range

$$5 \lesssim \Gamma_\gamma(24.7) \lesssim 14 \text{ kev}, \quad (5)$$

the greater uncertainty in the width of the 24.7-Mev resonance is due to the small branching ratio to the N^{15} ground state for this resonance combined with a rather large discrepancy in the measured^{8,9} branching ratio. (For these reasons the method used here is probably not the most accurate method of estimating the radiation width of the 24.7-Mev resonance.)

The estimates (4) and (5) are in qualitative agreement, at least as to order of magnitude, with the shell-model predictions of Elliott and Flowers and of Pal.

ACKNOWLEDGMENTS

We wish to acknowledge the warm encouragement of Professor R. Sherr in this investigation and the assistance of Mr. D. G. Fong in the analysis of the data. One of us (E. K. W.) is indebted for a correspondence with G. Morpurgo. Two of the authors (S. G. C. and P. S. F.) are grateful to the State Department for Fulbright travel grants, and one of the authors (S. G. C.) wishes to express his appreciation for the hospitality extended by the Palmer Physical Laboratory during his sabbatical leave in 1959.